Changes in microbubble dynamics near a boundary revealed by combined optical micromanipulation and high-speed imaging

V. Garbin,[a] D. Cojoc, E. Ferrari,[a] and E. Di Fabrizio[b]
CNR-INFM, TASC National Laboratory, S.S. 14 km 163.5, 34012 Basovizza, Trieste, Italy

M. L. J. Overvelde, S. M. van der Meer, N. de Jong,[c] D. Lohse, and M. Versluis
Physics of Fluids, University of Twente, P.O. Box 217, 7500 AE Enschede, The Netherlands

(Received 17 January 2007; accepted 6 February 2007; published online 13 March 2007)

The authors report optical observations of the change in the dynamics of one and the same ultrasound contrast agent microbubble due to the influence of interfaces and neighboring bubbles. The bubble is excited by a 2.25 MHz ultrasound burst and its oscillations are recorded with an ultrahigh-speed camera at 15 million frames per second. The position of an individual bubble relative to a rigid wall or second bubble is precisely controlled using optical tweezers based on Laguerre-Gaussian laser beams [P. Prentice *et al.*, Opt. Express **12**, 593 (2004); V. Garbin *et al.*, Jpn. J. Appl. Phys. **44**, 5773 (2005)]. This allows for repeated experiments on the very same bubble and for a quantitative comparison of the effect of boundaries on bubble behavior. © *2007 American Institute of Physics*. [DOI: 10.1063/1.2713164]

Micron-sized gas bubbles are effectively used as a contrast agent in ultrasound medical imaging. They contain an inert gas and are encapsulated by a phospholipid, protein, or polymeric shell. In the ultrasound field, with typical medical imaging frequencies between 1 and 10 MHz, they undergo linear and nonlinear oscillations, leading to an acoustical response that allows the discrimination of the blood pool from the surrounding tissue.[1] The study of the acoustical response of ultrasound contrast agent (UCA) microbubbles has attracted wide interest from both the medical and acoustical communities, not only for providing a better understanding of their complex dynamics, but also for their potential use for drug delivery and therapeutic applications.[2] Bubble oscillations at ultrasound frequencies can be recorded optically[3–5] with the advantage of providing direct visualization of nonlinear oscillations,[6] bubble rupture,[7] and interactions with vesicles or cells.[8,9] In our experiments, ultrahigh-speed optical imaging is performed using a digital rotating mirror camera specifically developed for investigating microbubble dynamics.[10] The camera system is capable of recording 128 frames at a frame rate of up to 25 million frames per second (Mfps), thereby fully resolving the oscillation dynamics at nanosecond time scale.

For molecular imaging applications in ultrasound, i.e., the noninvasive detection of a specific disease at a molecular level, it will be crucial to develop methods to selectively detect adherent UCA microbubbles that have bound to specific molecular targets from freely flowing ones, primarily based on a change in their acoustic response. Considerable differences in the amplitude of oscillations[11,12] and in the spectral response[13] were reported recently. In general, the studies on UCA microbubble dynamics suffer from the lack of control on bubble position, and they are therefore based on ensemble averaging and statistical observations of many different bubbles. Time-resolved dynamics of one and the same UCA microbubble under controlled well-defined conditions has not been reported previously.

In this letter, we report the use of optical tweezers for UCA microbubble manipulation, enabling the study of bubble dynamics with controlled boundary conditions. A quantification of the acoustical and fluid dynamical forces for the very same bubble when it is freely floating and when it is close to a boundary is therefore feasible, provided that the initial bubble properties remain unchanged in consecutive experiments. Three-dimensional optical trapping of single and multiple UCA microbubbles has been demonstrated by various groups, either by focusing an optical vortex beam, e.g., a Laguerre-Gaussian beam,[14,15] or by rapidly scanning the beam in a circular trajectory.[16] The ability to position UCA microbubbles with optical tweezers was also exploited for studying cell sonoporation phenomena induced by violently collapsing microbubbles.[17]

The setup for combined optical trapping and ultrahigh-speed imaging is based on an upright microscope (BXFM, Olympus), see Fig. 1. A Gaussian beam from a 1064 nm continuous wave Yb fiber laser (YLM, IPG Photonics) is converted into a Laguerre-Gaussian (LG) mode by a phase diffractive optical element[15] (DOE) implemented on a spatial light modulator (SLM) (X8267-11, Hamamatsu). Upon reflection on the dichroic mirror, the beam is focused by a 100× microscope objective (LUMFPL, Olympus; NA =1.00, water immersion) into an OptiCell cell culture chamber (BioCrystal, Inc.), where bubbles are injected. The beam divergence is adjusted to compensate for the mismatch between the trapping plane and the image plane. The chamber is positioned on top of a water-filled container with an unfocused 2.25 MHz transducer (V306, Panametrics Inc.) mounted at 45° incidence angle with the optical axis. A function generator (33120A, Agilent) was used to produce the driving pulse, which was then amplified by a RF power amplifier (350L, ENI). The acoustical beam (5 mm diameter) fully overlaps the optical field of view ($100\times100\ \mu m^2$). Bright-field transmission imaging is performed through the

[a]Also at: Department of Physics, University of Trieste, v. Valerio 2, 34127 Trieste, Italy.
[b]Present address: "Magna Græcia" University of Catanzaro, v.le Europa, 88100 Germaneto (CZ), Italy.
[c]Also at: Experimental Echocardiography, Thoraxcentre, Erasmus MC, Rotterdam, The Netherlands.

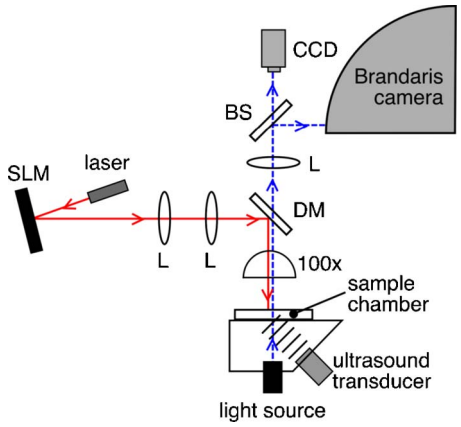

FIG. 1. (Color online) Setup for combined UCA microbubble trapping, acoustical driving, and ultrahigh speed optical recordings. The laser beam is converted by the spatial light modulator (SLM) into a Laguerre-Gaussian mode; upon reflection on a dichroic mirror (DM), it enters the objective (100×) and is focused into the sample volume. The ultrasound beam overlaps the optical focal volume. Beam splitter (BS) enables two imaging modes: monitor mode on a CCD camera (T=20%) and imaging mode on the ultrahigh speed camera Brandaris (R=80%). L: lenses.

same objective. A charge-coupled device (CCD) camera (LCL-902HS, Watec, 6% efficiency at 1000 nm) monitors the trapping beam shape and position, and the bubble selected to be trapped. The trapped bubble can be positioned at a prescribed distance from the wall by positioning the chamber upwards with 0.5 μm accuracy, using a micropositioning stage. The ultrahigh-speed camera is directly connected to the imaging port of the microscope and records the bubble oscillations during ultrasound insonation at 15 Mfps.

The dynamic implementation of DOEs on a programmable spatial light modulator enables fully flexible trap configurations. The size of a trap can be controlled by changing the Laguerre-Gaussian mode[18] and adapted to the full range of UCA microbubble sizes. All studies were performed with the experimental contrast agent BR-14 (Bracco Research S.A., Geneva), an agent containing phospholipid-stabilized microbubbles with a perfluorobutane gas core. The bubbles have a mean radius of 1.5 μm and 95% of the bubbles are smaller than 10 μm.

The insonifying ultrasound wave consists of an eight-cycle burst at a frequency of 2.25 MHz, with a peak negative pressure of 150–200 kPa (M.I.=0.12). The laser was momentarily blocked, and only during the recording, to avoid interfering optical forces and short enough for the bubble to remain in the trapped position, with the purpose that additional experiments could be repeated on the same bubble. For analysis and comparison with theoretical models, the two-dimensional bubble contours (which are always observed to be symmetrical in our experiments) were processed to track the bubble radius as a function of time, resulting in a so-called radius-time (R-t) curve of the bubble.

We investigated the influence of the chamber wall on the dynamics of an individual bubble. The radius-time curves of a bubble with a resting radius of R_0=2.45 μm are shown in Fig. 2. First, a movie was recorded when the bubble was insonified and positioned at the wall, while a second movie was recorded when the bubble was positioned 50 μm away from the wall. One last movie was recorded after positioning the bubble back at the wall to double-check if the bubble properties were not changed during the previous insonations.

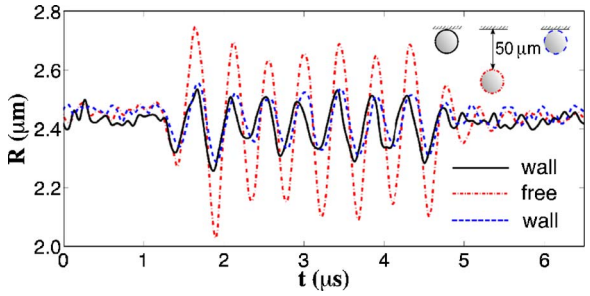

FIG. 2. (Color online) Three R-t curves of a single bubble with an initial radius R_0=2.45 μm, insonified with an eight-cycle ultrasound burst at 2.25 MHz with an applied pressure of 200 kPa. The frame rate is 15 Mfps. The solid line represents the amplitude of oscillations at the wall; the dash-dotted line is recorded with the bubble at a distance of 50 μm from the wall. The radius-time curve of the same bubble repeated at the wall identical (dashed line) is identical to the first one, showing that repeated insonations have not altered the initial bubble properties.

The radius-time curves indicate that the vicinity of the wall suppresses the amplitude of oscillations for one and the same microbubble by more than 50%. This finding can be attributed to three distinct effects. First, the vicinity of a rigid wall is expected to cause a shift in the resonance frequency of the bubble.[19] The effect of a rigid wall is commonly described by the so-called method of images (see, e.g., Refs. 20 and 21), where an acoustic image bubble is located in the mirrored position; a system of two bubbles having the same size and oscillating in phase indeed generates the same potential flow near the wall. As our experiments were carried out at a fixed insonation frequency of 2.25 MHz, a shift in the resonance frequency results in different amplitudes of oscillations being observed at the wall and away from the wall. Second, a full description of the bubble-wall system has to account also for a dissipation introduced by the viscous boundary layer at the wall, which is not taken into account when applying the image bubble method. This phenomenon contributes to the damping of the oscillations, in addition to the other damping mechanisms for coated bubbles (bulk and shell viscosity, thermal diffusion, and reradiation of sound). Finally, asymmetric oscillations may arise in the vicinity of the wall. The eccentricity of bubbles in the vicinity of a capillary wall and driven at comparable pressures has indeed been reported to be close to 0.7,[11] although these observations were made on adherent bubbles. In our experiments, the possible adhesion to the wall was excluded by verifying with the optical tweezers whether bubbles were indeed nonadherent, yet in contact with the wall. In order to visualize asymmetric oscillations, the behavior in a plane orthogonal to the wall should be observed; however, this was not possible in our present setup without major modifications.

The optical tweezers setup presented here, nonetheless, allows decoupling of the mechanisms listed above. The resonance frequency shift induced by the image bubble can be observed by studying a real two-bubble system. Then the viscous boundary layer induced by the wall is not present. Furthermore, in this case, the system is imaged in the plane containing both bubbles. Should asymmetric oscillations arise, they would then be detected from this point of observation. Two-trap DOEs are produced by dividing the full SLM active area into two sections, each containing a DOE for a single trap. The distance between the two traps can be controlled in realtime with submicrometer precision by changing the distance between the two DOEs, with a mini-

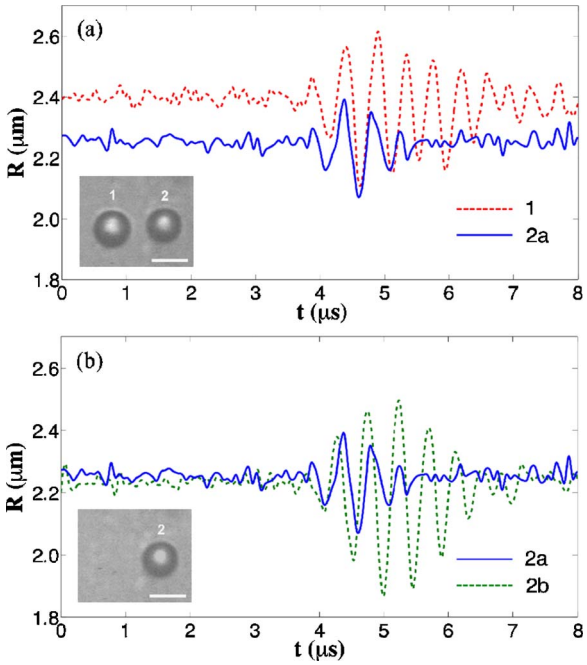

FIG. 3. (Color online) Radius-time curves taken at 15 Mfps for two interacting bubbles. (a) *R-t* curves of the two bubbles trapped at 8 μm distance from each other and positioned 50 μm away from the wall. The dashed curve 1 corresponds to bubble 1, the solid line 2a corresponds to bubble 2. (b) The dashed line 2b represents the *R-t* curve of bubble 2 oscillating after bubble 1 has been released. The *R-t* curve 2a is also plotted for comparison. White scalebar in pictures: 5 μm.

mum distance corresponding to the two bubbles being in contact and a maximum distance corresponding to several bubble diameter separation between the bubbles. The same approach can be used to efficiently generate larger arrays of traps (up to 10–20 in our setup), each one individually tuned for a prescribed bubble size.

Two bubbles having similar size were trapped with a separation distance in the same order as their diameter. The bubble pair was then positioned 50 μm away from the wall to reduce wall effects, as previously discussed, and to extract information purely on the bubble-bubble interaction. We investigated the radial dynamics of the bubble pair, then released one bubble by switching off the corresponding trap, and studied the behavior of the remaining bubble.

Figure 3 shows the result of this experiment: the initial radii of the bubbles are 2.25 and 2.40 μm, respectively, the bubble centers being 8 μm apart. The dynamics of the bubble pair in ultrasound (f=2.25 MHz, P_a=150 kPa) was first recorded at 15 Mfps, see the radius-time curves of Fig. 3(a). In Fig. 3(b) the radius-time curve for the residual bubble is shown together with the radius-time curve previously recorded for the very same bubble in the presence of the second one. When comparing the two curves, it is apparent that bubble oscillations are highly suppressed by the presence of the neighboring bubble. In repeated experiments, the two bubbles always retained their spherical symmetry. In this case, we can thus ascribe the change in the bubble response to the shift in resonance frequency. A change in the distance between the bubbles was also observed (data not presented here) due to an attractive secondary Bjerknes force (see, e.g., Ref. 20 for an overview of the topic), a detailed study and quantification of which will be the subject of a forthcoming paper.

In this letter we presented a setup that enables for a quantitative characterization of the boundary-dependent UCA microbubble dynamics at the single-bubble level. We compared the behavior of the very same UCA microbubble under different boundary conditions by a well-controlled positioning of individual bubbles using Laguerre-Gaussian optical tweezers and by recording their ultrasound-driven oscillations with an ultrahigh-speed camera. We therefore introduced a powerful tool for investigating how the bubble dynamics, hence the acoustical signature, changes with varying distance to neighboring objects. A deeper understanding of these phenomena may lead to improved imaging modalities together with the use of functionalized microbubbles specifically designed for targeted diagnostic ultrasound imaging.

The authors thank M. Arditi and P. J. A. Frinking of Bracco Research S.A. (Geneva) for initiating this work and for helpful comments. One of the authors (V.G.) thanks Bracco Imaging (Milan) for financial support.

[1] B. B. Goldberg, J. Raichlen, and F. Forsberg, *Ultrasound Contrast Agents: Basic Principles and Clinical Applications*, 2nd ed. (Dunitz, London, 2001).
[2] J. R. Lindner, Nat. Rev. Drug Discovery **3**, 527 (2004).
[3] J. Chomas, P. Dayton, D. May, J. Allen, A. Klibanov, and K. Ferrara, Appl. Phys. Lett. **77**, 1056 (2000).
[4] N. de Jong, P. Frinking, A. Bouakaz, M. Goorden, T. Schourmans, X. Jingping, and F. Mastik, Ultrasound Med. Biol. **26**, 487 (2000).
[5] N. Kudo, T. Miyaoka, K. Kuribayashi, and K. Yamamoto, J. Acoust. Soc. Am. **108**, 2547 (2000).
[6] P. Marmottant, S. van der Meer, M. Emmer, M. Versluis, N. de Jong, S. Hilgenfeldt, and D. Lohse, J. Acoust. Soc. Am. **118**, 3499 (2005).
[7] A. Bouakaz, M. Versluis, and N. de Jong, Ultrasound Med. Biol. **31**, 391 (2005).
[8] P. Marmottant and S. Hilgenfeldt, Nature (London) **243**, 153 (2003).
[9] C.-D. Ohl, M. Arora, R. Ikink, N. de Jong, M. Versluis, M. Delius, and D. Lohse, Biophys. J. **91**, 4285 (2006).
[10] C. T. Chin, C. Lancée, J. Borsboom, F. Mastik, M. E. Frijlink, N. de Jong, M. Versluis, and D. Lohse, Rev. Sci. Instrum. **74**, 1 (2003).
[11] S. Zhao, K. W. Ferrara, and P. A. Dayton, Appl. Phys. Lett. **87**, 134103 (2005).
[12] M. Lankford, C. Z. Behm, J. Yeh, A. L. Klibanov, P. Robinson, and J. Linder, Invest. Radiol. **41**, 721 (2006).
[13] S. Zhao, D. E. Kruse, K. W. Ferrara, and P. A. Dayton, J. Acoust. Soc. Am. **120**, EL63 (2006).
[14] P. Prentice, M. MacDonald, T. Frank, A. Cuschieri, G. Spalding, W. Sibbett, P. Campbell, and K. Dholakia, Opt. Express **12**, 593 (2004).
[15] V. Garbin, D. Cojoc, E. Ferrari, R. Z. Proietti, S. Cabrini, and E. Di Fabrizio, Jpn. J. Appl. Phys., Part 1 **44**, 5773 (2005).
[16] P. H. Jones, E. Stride, and N. Saffari, Appl. Phys. Lett. **89**, 081113 (2006).
[17] P. Prentice, A. Cuschieri, K. Dholakia, M. Prausnitz, and P. Campbell, Nat. Phys. **1**, 107 (2005).
[18] M. J. Padgett and L. Allen, Opt. Commun. **121**, 36 (1995).
[19] M. Strasberg, J. Acoust. Soc. Am. **25**, 536 (1953).
[20] T. G. Leighton, *The Acoustic Bubble* (Academic, London, 1994).
[21] C. E. Brennen, *Cavitation and Bubble Dynamics* (Oxford University Press, New York, 1995).